


Exome sequencing in syndromic brain malformations identifies novel mutations in *ACTB*, and *SLC9A6*, and suggests *BAZIA* as a new candidate gene

Valerie Weitensteiner^{1*} | Rong Zhang^{1,2*} | Julia Bungenberg³ | Matthias Marks⁴ | Jan Gehlen^{1,2} | Damian J. Ralser¹ | Alina C. Hilger^{1,5} | Amit Sharma⁶ | Johannes Schumacher^{1,2} | Ulrich Gembruch⁷ | Waltraut M. Merz⁷ | Albert Becker³ | Janine Altmüller^{8,9} | Holger Thiele⁸ | Bernhard G. Herrmann⁴ | Benjamin Odermatt¹⁰ | Michael Ludwig¹¹ | Heiko Reutter^{1,2,12} 

¹Institute of Human Genetics, University of Bonn School of Medicine and University Hospital of Bonn, Bonn, Germany

²Department of Genomics—Life & Brain Center, Bonn, Germany

³Department of Neuropathology, University of Bonn, Bonn, Germany

⁴Department of Developmental Genetics, Max-Planck-Institute for Molecular Genetics, Berlin, Germany

⁵Department of Pediatrics, University of Bonn, Bonn, Germany

⁶Department of Neurology, University Clinic Bonn, Bonn, Germany

⁷Department of Obstetrics and Prenatal Medicine, University of Bonn, Bonn, Germany

⁸Cologne Center for Genomics, University of Cologne, Cologne, Germany

⁹Center for Molecular Medicine Cologne, University of Cologne, Cologne, Germany

¹⁰Institute of Anatomy, University of Bonn, Bonn, Germany

¹¹Department of Clinical Chemistry and Clinical Pharmacology, University of Bonn, Bonn, Germany

¹²Department of Neonatology and Pediatric Intensive Care, Children's Hospital, University of Bonn, Bonn, Germany

Correspondence

Heiko Reutter, Department of Neonatology and Pediatric Intensive Care and Institute of Human Genetics, University of Bonn, Sigmund-Freud-Str. 25, 53105 Bonn, Germany.
Email: reutter@uni-bonn.de

Present address

Matthias Marks, Matthias Marks, Department of Neurobiological, Research RWTH Aachen University, Aachen, Germany

Funding information

V.W. is supported by the BONFOR program of the University of Bonn (grant number O-149.0105.1). A.C.H. is

Background: Syndromic brain malformations comprise a large group of anomalies with a birth prevalence of about 1 in 1,000 live births. Their etiological factors remain largely unknown. To identify causative mutations, we used whole-exome sequencing (WES) in aborted fetuses and children with syndromic brain malformations in which chromosomal microarray analysis was previously unremarkable.

Methods: WES analysis was applied in eight case-parent trios, six aborted fetuses, and two children.

Results: WES identified a novel *de novo* mutation (p.Gly268Arg) in *ACTB* (Baraitser-Winter syndrome-1), a homozygous stop mutation (p.R2442*) in *ASPM* (primary microcephaly type 5), and a novel hemizygous X-chromosomal mutation (p.I250V) in *SLC9A6* (X-linked syndromic mental retardation, Christianson type). Furthermore, WES identified a *de novo mutation* (p.Arg1093Gln) in *BAZIA*. This mutation was previously reported in only one allele in 121,362 alleles tested (dbSNP build 147). *BAZIA* has been associated with neurodevelopmental impairment and

*These authors contributed equally to this work.

supported by the BONFOR program of the University of Bonn (grant number O-149.0123). H.R. and ML are supported by grant RE 1723/1-1 from the German Research Foundation (Deutsche Forschungsgemeinschaft, DFG). B.O. is funded by a repatriation grant from the North Rhine–Westphalian Ministry of Innovation, Science, and Research. HR is also supported by a grant of the Else-Kröner-Fresenius-Stiftung (EKFS; funding code 2014_A14). The authors have no conflict of interest to declare.

dysregulation of several pathways including vitamin D metabolism. Here, serum vitamin-D (25-(OH)D) levels were insufficient and gene expression comparison between the child and her parents identified 27 differentially expressed genes. Of note, 10 out of these 27 genes are associated to cytoskeleton, integrin and synaptic related pathways, pinpointing to the relevance of *BAZIA* in neural development. *In situ* hybridization in mouse embryos between E10.5 and E13.5 detected *Baz1a* expression in the central and peripheral nervous system.

Conclusion: In syndromic brain malformations, WES is likely to identify causative mutations when chromosomal microarray analysis is unremarkable. Our findings suggest *BAZIA* as a possible new candidate gene.

KEYWORDS

BAZIA, brain malformations, in situ hybridization, VATER/VACTERL association, whole-exome sequencing

1 | INTRODUCTION

Syndromic brain malformations comprise a large group of congenital anomalies with a birth prevalence of 1 in 1,000 live births (Chitty & Pilu, 2009). The phenotypical spectrum is polymorphic and clinical symptoms vary from global developmental delay and intellectual disability to mild attention deficits (Poretti, Boltshauser, & Huisman, 2014). Despite of an overall improvement in medical care over the past decades, brain malformations constitute still an important source of chronic disability in the affected children. While an ongoing progress in neuroimaging and prenatal ultrasound diagnostics has improved diagnostic procedures, no effective therapy for the associated neurocognitive impairments is available to date and their etiology remains elusive in the majority of cases (Kalter & Warkany, 1983). Among the known genetic factors are numeric chromosomal abnormalities (e.g., trisomy 13, 18), structural microscopic and submicroscopic chromosomal anomalies (e.g., Miller-Dieker lissencephaly syndrome; MIM #247200) or monogenic recessive or dominant inherited syndromes (e.g., Joubert syndrome or holoprosencephaly type 3) (Jeng, Tarvin, & Robin, 2001). Lately, the systematic application of high-throughput molecular genetics, such as chromosomal microarray analysis and more recently whole-exome sequencing (WES), led to the identification of more novel disease-causing copy number variations (CNVs) (De Wit et al., 2014; Hillman et al., 2013; Kariminejad et al., 2011; Krutzke et al., 2016; Sajjan et al., 2013; Schumann et al., 2016; Wapner et al., 2012) and disease-causing biallelic recessive, respectively heterozygous dominant mutations for brain malformations, than ever before (Aldinger et al., 2014; Mishra-Gorur et al., 2014). Here, we used a family based whole-exome sequencing (WES) approach to identify causative mutations in eight case-parent trios (six aborted fetuses and two children) with syndromic brain malformations. In all of these eight cases

chromosomal microarray analysis was carried out prior to WES and was found to be unremarkable.

2 | MATERIALS AND METHODS

2.1 | Patients, controls, and DNA isolation

The study was conducted in accordance with the Declaration of Helsinki, and ethical approval was obtained from the local ethic committee (reference numbers 208/08 & 009/09). Written informed consent was obtained from parents prior to study entry. In the format of written and signed forms, all participating subjects or their legal guardians agreed on the publication of the study results.

In our study, we included six fetuses with syndromic brain malformations, which had been sampled through the Department of Obstetrics and Prenatal Medicine at the University of Bonn. Furthermore, we added two children syndromic brain malformations sampled through the German self-help organization for individuals with anorectal malformations (SoMA e.V.) and one of the authors (H.R.). A detailed phenotype description of these cases is given in Table 1. In all cases, parental DNA could be obtained. There was an unremarkable family history in all cases. Prior to this study, all case-parent trios underwent chromosomal microarray analysis to rule out disease-causing CNVs (Dworschak et al., 2015; Krutzke et al., 2016). Genomic DNA was isolated from whole blood using the Chemagic DNA Blood Kit special (Chemagen, Baesweiler, Germany). Genomic DNA from saliva samples was isolated with the Oragene DNA Kit (DNA Genotek Inc., Kanata, Canada).

2.2 | Whole-exome sequencing and data analysis

For enrichment of genomic DNA we used the NimbleGen SeqCap EZHumanExome Library v2.0 enrichment kit. For

TABLE 1 Phenotype of fetuses and patients investigated by whole-exome sequencing

| Case (age and sex) | CNS malformation/anomaly | Additional features/anomalies |
|--|---|---|
| Case 1 <ul style="list-style-type: none"> • 20 + 0 weeks of gestation • Male fetus | <ul style="list-style-type: none"> • Hydrocephalus | Left-sided cleft lip and palate, low set ears, hypertelorism, single umbilical artery, bilateral renal pyelectasis, nuchal edema |
| Case 2 <ul style="list-style-type: none"> • 11 years of age • Female patient | <ul style="list-style-type: none"> • Partial agenesis of corpus callosum • Absent septum pellucidum | Pyloric atresia, anorectal malformation with vestibular fistula, left-sided renal agenesis, right-sided pancake kidney, atrial and ventricular septal defects, butterfly vertebrae, tethered cord, and bilateral thumb hypoplasia (VATER/VACTERL association) |
| Case 3 <ul style="list-style-type: none"> • 34 + 0 weeks of gestation • Female fetus | <ul style="list-style-type: none"> • Hydrocephalus • Macrocephaly | Right-sided microphthalmia and kryptophthalmia, aortic isthmus stenosis, absent lobulation of the left lung, and hypoplastic pancreas |
| Case 4 <ul style="list-style-type: none"> • 8 years of age • Male patient | <ul style="list-style-type: none"> • Hydrocephalus • Thoracic syringomyelia | Anorectal malformation with rectourethral fistula, esophageal atresia, vertebral and costal malformation, dextro-versio cordis, left-sided multicystic dysplastic kidney, hypospadias, right-sided radial and thumb aplasia, left-sided thumb hypoplasia |
| Case 5 <ul style="list-style-type: none"> • 27 + 4 weeks of gestation • Female fetus | <ul style="list-style-type: none"> • Schizencephaly • Microcephaly • Lobar holoprosencephaly | |
| Case 6 <ul style="list-style-type: none"> • 24 + 6 weeks of gestation • Female fetus | <ul style="list-style-type: none"> • Microcephaly • Pachygyria | |
| Case 7 <ul style="list-style-type: none"> • 20 + 5 weeks of gestation • Male fetus | <ul style="list-style-type: none"> • Hydrocephalus • Agenesis of the vermis | |
| Case 8 <ul style="list-style-type: none"> • 33 + 5 weeks of gestation • Female fetus | <ul style="list-style-type: none"> • Holoprosencephaly | |

WES a 100bp paired-end read protocol was used according to the manufacturer's recommendations on an Illumina HiSeq2000 sequencer by the Cologne Center for Genomics (CCG), Cologne, Germany. Data analysis and filtering of mapped target sequences was performed with the 'Varbank' exome and genome analysis pipeline v.2.1 (unpublished; <https://varbank.ccg.uni-koeln.de>, see Supporting Information Table 1). Mutations, unclassified variants, and phenotype data were submitted to the ClinVar, NCBI database (<http://www.ncbi.nlm.nih.gov/clinvar/>).

2.3 | Confirmation of variants detected by WES

Variations identified by WES and called to be likely causative were amplified from DNA by polymerase chain reaction (PCR), and automated sequence analysis was carried out using standard procedures. In brief, primers were directed to all six variations observed and the resultant PCR products were subjected to direct automated BigDye Terminator sequencing (3130XL Genetic Analyzer, AppliedBiosystems,

FosterCity, California, USA). Both strands from each amplicon were sequenced and presence of the variations in each trio was investigated by sequencing the respective PCR product.

2.4 | Exon trap analysis

To obtain sufficient amounts of DNA, we first performed “whole genome amplification” of fetal DNA. We cloned genomic wild type sequence of *ACTB* exon 3–5 and sequence bearing the potential splice-site mutation into the “Exon Trap Cloning Vector” pET01 (MoBiTec, Göttingen, Germany). Primers used for cloning are: ACTBclonef_XhoI: atagtactcgagCCCAGGCACCAGGTAGG; ACTBcloneR_NotI: ttgtagcggccgcCACACCACAGGACCCAC. In a next step, HEK293T cells (European Collection of Cell Cultures [ECACC]) were transiently transfected using Lipofectamine 2000 (Invitrogen, Paisley, UK) according to the manufacturer’s protocol. Cells were collected after 48 h and total RNA was isolated using Dynabeads mRNA DIRECT Micro Kit (Life Technologies AS, Oslo). After reverse transcription into cDNA using High Capacity cDNA Reverse Transcription Kit (Applied Biosystems, Foster City, CA), complementary DNA was amplified by standard PCR. The PCR products were visualized by gel electrophoresis, purified (Wizard SV Gel and PCR Clean-up System; Promega, Mannheim, Germany) and sequenced by Sanger sequencing.

2.5 | RNA extraction

Whole blood samples were collected using PAXgeneTM Blood RNA Tubes (PreAnalytiX, Hombrechtikon, Switzerland). PAXgene TM Blood RNA Tubes enable immediate stabilization of intracellular RNA. Isolation and purification of total RNA from whole blood was carried out by using PAXgene Blood miRNA Kit (PreAnalytiX, Switzerland). DNase digestion was included in the isolation and purification steps.

2.6 | mRNA sequencing and data analysis in patient 2 and his parents

RNA sequencing was performed with QuantSeq-3'-mRNA-Seq Library Preparation kit (Lexogen, Vienna, Austria) according to the manufacturer’s protocols and 50 bp single reads were generated with an Illumina HiSeq 2500 RapidRun. Raw reads were subjected to quality and adapter trimming with TrimGalore! (http://www.bioinformatics.babraham.ac.uk/projects/trim_galore/) (–quality 20). Then, the reads were aligned to GRCh37p13 with Subread (-d 45 -M 14 -u) (Liao, Smyth, & Shi, 2013). Subsequent expression quantification was performed with featureCounts (-d 45)

(Liao, Smyth, & Shi, 2014) with the Ensembl annotation GRCh37.82.

To reduce the burden of multiple testing, we excluded the hemoglobin genes (<http://www.genenames.org/cgi-bin/genefamilies/set/940>) and Ensembl gene identifiers with no corresponding HGNC symbol (Gray, Yates, Seal, Wright, & Bruford, 2015) and kept only those annotated as protein coding via the R-package biomaRt (Durinck, Spellman, Birney, & Huber, 2009). Genes with less than 2 counts per million were filtered out. In total 9 million counted reads were subjected to differential gene expression analysis with edgeR (Robinson, McCarthy, & Smyth, 2010) according to the user guide.

2.7 | Vitamin D analysis

Assays for serum vitamin-D levels were as follows: 25-OH-vitamin D was determined by a chemiluminescence immunoassay (CLIA; ABBOTT Diagnostics Division, Wiesbaden, Germany). Calcitriol (1,25-dihydroxyvitamin D₃) was measured by CLIA (IDS isys, Immunodiagnostiksystems, UK).

2.8 | In situ hybridization of mouse whole embryos (WISH)

All mice experiments were performed in accordance with the revised Animals Directive 2010/63/EU in Europe using state-of-the-art transgenic mouse technologies at the Department of Developmental Genetics, Max-Planck-Institute for Molecular Genetics, Berlin, Germany.

Wild-type embryos of the NMRI mouse strain were dissected at embryonic day (E) 10.5, 12.5, and 13.5. Processing of the embryos, in vitro transcription of the RNA antisense probe, and WISH were performed according to the protocols provided on the MAMEP homepage (<http://mamep.molgen.mpg.de>) with slight modifications. As template for the *Baz1a* probe, the MAMEP clone 9230 was used. Staining reaction was done using BM Purple (Roche). Images were taken using a MZ 16A dissection microscope (Leica) in combination with an AxioCam MRc5 camera and the AxioVision software (Carl Zeiss MicroImaging). At least 3 embryos per stage were analyzed and representative embryos are shown.

2.9 | In silico prediction methods

To predict the disease-causing potential of the variants identified, we used the following programs: Polyphen2 (<http://genetics.bwh.harvard.edu/pph2/>), MutationTaster (<http://www.mutationtaster.org>), SIFT (http://sift.jcvi.org/www/SIFT_chr_coords_submit.html), MutPred (<http://mutpred.mutdb.org>) and PROVEAN (<http://provean.jcvi.org/index.php>).

3 | RESULTS

WES data analysis in all eight case-parent trios detected 10 putative *de novo* variants in 10 different genes in 5 different case-parent trios (Case 1, Case2, Case 3, Case 6, and Case 7). Furthermore, WES data analysis identified one likely causative homozygous autosomal, and one likely causative hemizygous X-chromosomal variant (Case 6 and Case 7). Sanger sequencing validated five of the 10 putative *de novo* variants in three case-parent trios (Case 1, Case 2, and Case 3) as well as the homozygous respectively hemizygous variant found in **Case 6** and Case 7. According to the “Exome Aggregation Consortium (ExAC; <http://exac.broadinstitute.org/>)” four of the identified variants were novel, one in *ACTB* found in Case1, one in *NBAS* found in Case 2, one in *ASPM* found in Case 6, and one in *SLC9A6* found in Case 7. All five *de novo* variants identified have been submitted to ClinVar (<http://www.ncbi.nlm.nih.gov/clinvar/>) and their significance was determined using five different online prediction tools as outlined above.

In Case 1, mutation analysis identified a novel *de novo* variant in *ACTB* (p.Gly268Arg). Case 1 was an aborted male fetus with hydrocephalus, left-sided cleft lip and palate, low set ears, hypertelorism, single umbilical artery, bilateral renal pyelectasis, and nuchal edema. Heterozygous mutations in *ACTB*, encoding actin cytoplasmic 1 protein, cause Baraitser-Winter syndrome-1 (BRWS1) (MIM #243310) (Baraitser & Winter, 1988; Rivière et al., 2012), a human malformation syndrome with complete phenotypic overlap to Case 1. In accordance, four out of five online prediction tools classified the mutation as disease-causing (Table 2). The identified mutation, p.Gly268Arg, substitutes a highly conserved small uncharged glycine with a basic arginine. Furthermore, this mutation resides at the end of exon 4 (c.802G > C) and lowers the consensus value (CV) for splice site recognition (CV:0.754 for GCgtgagt), compared to the wild type sequence (CV:0.888 for GGgtgagt) (Shapiro & Senapathy, 1987). To further characterize a possible splice site recognition effect, we employed “Exon Trapping” (Duyk, Kim, Myers, & Cox, 1990). However, this did not reveal any affection of the splicing process (Supporting Information Fig. 1). While the disease-causing mechanism of the identified mutation remains uncertain, the phenotypic overlap of Case 1 with BRWS1 and the *de novo* status of the mutation suggest it to be disease-causing.

In Case 2, mutation analysis identified two heterozygous *de novo* variants in *NBAS* (neuroblastoma amplified sequence) (p.Thr1424Ile), and in *BAZIA* (p.Arg1093Gln), encoding the ATP-utilizing chromatin assembly and remodeling factor 1 (ACF1), respectively. At the time of assessment, Case 2 was an 11 year old girl with partial agenesis of the corpus callosum, absent septum pellucidum, pyloric

TABLE 2 Identified and confirmed *de novo* mutations and their prediction program outcome

| Case | Gene | Transcript ID | c.Change | p.Change | dbSNP (build147) | Polyphen2 | Mutation Taster | SIFT | MutPred | PROVEAN |
|------|--------------|-----------------|-----------|--------------|------------------------------|-------------------------|------------------------|---------------------------|-------------------|----------------------|
| 1 | <i>ACTB</i> | ENST00000331789 | c.802G>C | p.Gly268Arg | Novel | Probably damaging (1.0) | Disease causing (0.99) | Not predicted | Deleterious (87%) | Deleterious (-8,000) |
| 2 | <i>NBAS</i> | ENST00000331789 | c.4271C>T | p.Thr1424Ile | Novel | Probably damaging (1.0) | Disease causing (0.99) | Not predicted | Deleterious (28%) | Deleterious (-2,799) |
| 2 | <i>BAZIA</i> | ENST00000382422 | c.3278G>A | p.Arg1093Gln | rs776556963 (MAF 0.00000824) | Probably damaging (1.0) | Disease causing (0.99) | Tolerated (0.21) | Deleterious (34%) | Neutral (-1,567) |
| 3 | <i>SCN9A</i> | ENST00000409672 | c.721T>A | p.Ser241Thr | rs80356470 (MAF not given) | Probably damaging (1.0) | Disease causing (0.99) | Damaging (low confidence) | Deleterious (89%) | Deleterious (-2,931) |
| 3 | <i>DLG3</i> | ENST00000374355 | c.64T>G | p.Ser22Ala | Novel | Benign (0.001) | Polymorphism (0.99) | Not predicted | Deleterious (38%) | Neutral (-0,557) |

MAF = minor allele frequency.

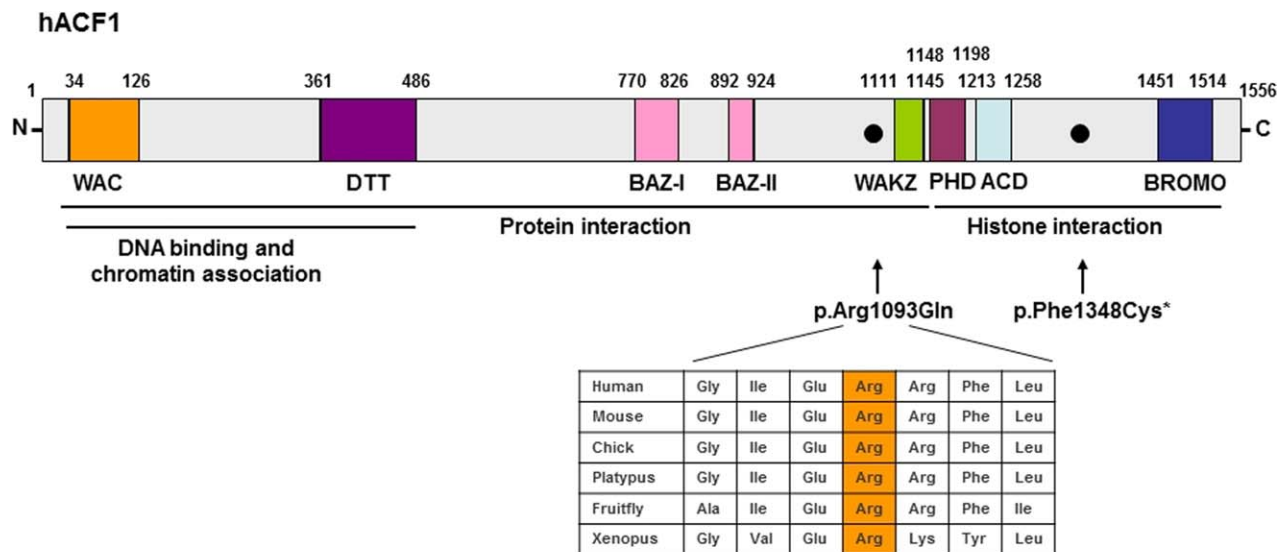


FIGURE 1 Schematic representation of human ACF1 protein adopted from Zaghlool et al. (2016). Known domains are drawn to scale with the corresponding amino acid residue numbers given above. Established interactions are shown below. Protein domains include a WAC and DTT motif, necessary for ACF1-DNA binding and chromatin association (Doerks, Copley, & Bork, 2001; Fyodorov & Kadonaga, 2002; Noguchi, Rapp, Skorobogatko, Bailey, & Noguchi, 2012). Three motifs, BAZ-I, BAZ-II and WAKZ (Jones, Hamana, Nezu, & Shimane, 2000) were shown to be involved in the assembly of the CHRAC1/POLE1 complex and in SMARCA5 and NCOR1 binding (Collins et al., 2002; Ewing et al., 2007; Kukimoto et al., 2004). The PHD finger (Aasland, Gibson, & Stewart, 1995; Jones et al., 2000) recognizes histone H3 peptide trimethylated at lysine 4 (H3K4me3) (Peña et al. 2006), whereas the bromodomain binds lysine-acetylated H3 or H4 (Zeng and Zhou, 2002). There is also evidence, that a domain rich in acidic residues (ACD) is also important for ACF1 histone interaction (Fyodorov & Kadonaga, 2002). The p.Arg1093Gln mutation identified resides in the linker region between the BAZ-II and WAKZ motifs and is depicted with a black dot in the protein (*also shown is the p.Phe1348Cys substitution identified by Zaghlool et al. (2016). Human ACF1 protein sequence and the evolutionary conservation of the mutated p.Arg1093 with its surrounding residues is shown from UniProtKB entries Q9NRL2, O88379, F1NFV8, F6PGF4, W8C5T1, and F7BSN0

atresia, anorectal malformation with vestibular fistula, left-sided renal agenesis, right-sided pancake kidney, atrial and ventricular septal defects, butterfly vertebrae (comprising Th6 and fused vertebrae comprising L4-S1), tethered cord with sacral lipoma, bilateral club feet, and bilateral thumb hypoplasia, resembling the extended spectrum of the VATER/VACTERL association with additional brain malformations.

Although, four out of five online prediction tools classified the identified mutation in *NBAS* as disease-causing (Table 2), only biallelic mutations in *NBAS* have been associated with disease in human, comprising a multisystem disease involving liver, eye, immune system, connective tissue, and bone (MIM #614800) (Maksimova et al., 2010). A more recent report associated biallelic mutations in *NBAS* with recurrent acute liver failure in infancy (MIM #616483) (Haack et al., 2015). So far, neither heterozygous missense nor heterozygous loss of function mutations in *NBAS* have been associated with any human disease. Hence, we did not account the identified novel *de novo* mutation p.Thr1424Ile in *NBAS* as disease-causing.

The *de novo* p.Arg1093Gln mutation in *BAZIA* has been previously reported in only one allele in 121.362 alleles tested (dbSNP build 147, August 2016; minor allele

frequency of 0.00000824; rs776556963). Three out of five online prediction tools classified the identified mutation in *BAZIA* as disease-causing (Table 2). The p.Arg1093Gln variant substitutes a basic arginine residue by a polar uncharged glutamine, and alters Kyte-Doolittle hydrophobicity values (−4.5 to −3.5) at this position (Kyte & Doolittle, 1982). However, a reliable modeling of the tertiary structure of this nonconservative exchange is not available yet, and prediction of the secondary structure provided no evidence for an effect on ACF1 folding (SOPMA SECONDARY STRUCTURE PREDICTION; <https://npsa-prabi.ibcp.fr>; data not shown). Nonetheless, Arg1093 resides in a highly conserved region in the vicinity of the WAKZ domain (residues 1111–1145) and this region is conserved to a great extent as far down as *Xenopus* and *Drosophila* (Figure 1).

To further assess the potential role of *BAZIA* in the formation of human malformations, as seen in Case 2, we investigated the expression of *Baz1a* by whole-mount in situ hybridization (WISH) on mouse embryos at embryonic days (E) 10.5 to 13.5. This time frame represents the equivalent of human gestational weeks 5–8 hence, the postulated time of VATER/VACTERL organogenesis in humans (Stevenson & Hunter, 2013) (Figure 2). Strong expression of *Baz1a* could be detected in VATER/VACTERL associated tissues, such

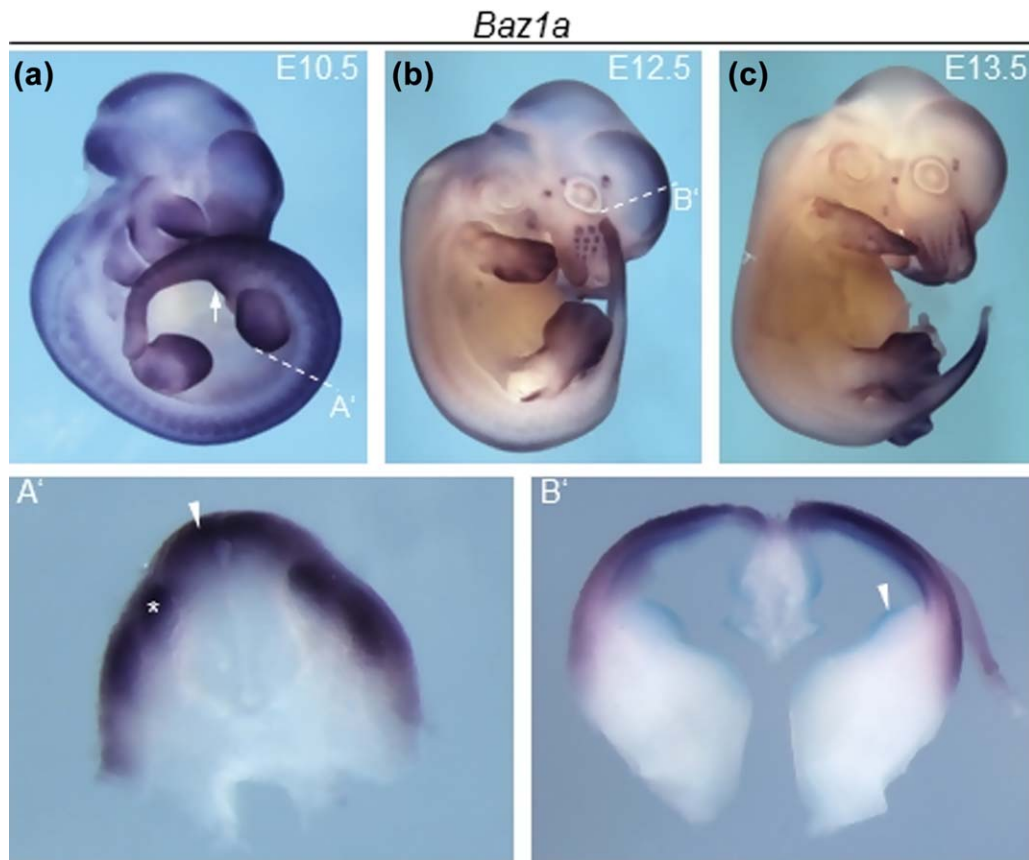


FIGURE 2 Whole mount *in situ* hybridization for *Baz1a* on E10.5 (a), E12.5 (b), and E13.5 (c) mouse embryos. Arrow in (A) highlights cloacal membrane expression of *Baz1a*. Dashed lines indicate section planes for tungsten needle sections through the trunk anterior of the hindlimb buds at E10.5 (A') and the telencephalon at E12.5 (B'). Asterisk in A' marks dorsal root ganglia, arrowhead *Baz1a* dorsal neural tube expression. The arrowhead in B' marks *Baz1a* expression in the ventricular layer

as the cloacal membrane (Figure 2a, arrow). Staining was also apparent in structures of the developing dorsal neural tube (Figure 2a/a'') matching the phenotypic spectrum of our patient with congenital tethered cord and sacral lipoma. Furthermore, staining was found in the ventricular layer of the telencephalon (Figure 2b/b'). In addition, *Baz1a* expression was detectable in dorsal root ganglia, the dermomyotome, and the surface ectoderm (Figure 2a'/b'). The latter showed domains of enrichment in the developing limbs matching also the phenotypic spectrum of our patient with bilateral congenital thumb hypoplasia, and we further found staining of the branchial arches, and the whisker pads (Figure 2a–c).

In Case 3, mutation analysis identified two *de novo* variants in *SCN9A* (p.Ser241Thr) and in *DLG3* (p.Ser22Ala). At the time of assessment, Case 3 was a female fetus with hydrocephalus, macrocephaly, right-sided microphthalmia and kryptophthalmia, aortic isthmus stenosis, absent lobulation of the left lung, and hypoplastic pancreas. The identified variant in *SCN9A*, encoding the sodium channel protein type 9 subunit alpha (Na_v1.7), has been previously reported in one singleton only, with no minor allele frequency given (rs80356470; dbSNP build 147, August 2016). All five online prediction tools classified the identified mutation in

SCN9A as disease-causing (Table 2) and Ser241 is absolutely conserved at its position in mammals and chicken. Since *SCN9A* has not been associated with formation of congenital malformations of any kind, we do not account the here identified mutation as disease-causing for the fetal phenotype of Case 3.

Besides the *de novo* mutation in *SCN9A* we identified a second novel *de novo* mutation, p.Ser22Ala in *DLG3*, encoding the X-chromosomal protein disks large homolog 3, a member of the membrane-associated guanylate kinase protein family. This amino acid residue is not included in the full-length protein and solely affects one short, amino-terminal deleted isoform (UniProtKB Q92796-2). Only one out of five online prediction tools classified the identified mutation in *DLG3* as disease-causing (Table 2). As the mutation carrying fetus was of female gender, we also tested for the skewedness of X-chromosome inactivation, but detected no abnormal X-chromosome inactivation (Supporting Information Fig. 2). Given all these findings, the here identified *de novo* mutation, p.Ser22Ala in *DLG3*, was not assumed to be involved in the etiology of the fetal phenotype.

In Case 6, mutation analysis identified a novel homozygous mutation (p.R2442*) in *ASPM* (primary microcephaly

type 5) (MIM #608716), leading to a premature stop. Case 6 was a female fetus with microcephaly and pachygyria on prenatal ultrasound showing marked phenotypic overlap to patients previously described with primary microcephaly type 5. To the best of our knowledge, these previously described compound heterozygous or homozygous mutations in *ASPM* have been exclusively loss of function mutations distributed over the complete coding region (Bond et al., 2003) arguing for the here identified homozygous stop mutation to be disease-causing in Case 6.

In Case 7, mutation analysis identified a novel hemizygous mutation (p.I250V) in *SLC9A6* (X-linked syndromic mentally retardation, Christianson type) (MIM #300243). Case 7 was a male fetus with hydrocephalus and agenesis of the vermis on prenatal ultrasound. Previous reports of male patients with disease-causing hemizygous mutations in *SLC9A6* show progressive postnatal cerebellar atrophy and microcephaly (Gilfillan et al., 2008). Pescosolido et al. (2014) investigating 14 boys with mutations in *SLC9A6* showed marked atrophy of the vermis in three of the 14 boys. Although, to the best of our knowledge, no report of prenatal diagnosis of X-linked syndromic mental retardation of Christianson type has been described in the literature, the fetus described here showed already agenesis of the vermis on prenatal ultrasound with an amino acid substitution in *SLC9A6* (c.748A > G) of a highly conserved position down to *Xenopus tropicalis* suggesting the mutation to be disease-causing in Case 7. Hence, Case 7 might expand the phenotypic spectrum of X-linked syndromic mental retardation of Christianson type in regards to manifestation into the prenatal period.

4 | DISCUSSION

The present study applied WES in six fetuses and two children with syndromic brain malformations in which chromosomal microarray analysis was previously unremarkable. WES identified causative mutations in three fetuses (Case 1, Case 6, and Case 7). Furthermore, our analysis suggests *BAZIA* as a new possible candidate gene for syndromic brain malformations (Case 2).

The finding of an *ACTB* amino acid substitution, p.Gly268Arg, *per se* should be responsible for the phenotype observed in Case 1. As outlined by Verloes, Drunat, Pilz, and Di Donato (2015), BRWS presents, amongst other features, with brain malformations, cleft lip and palate, as well as anomalies of the eye, ear, and the renal tract, hence the complete spectrum found in Case 1. Similarly, the phenotypic spectrum previously described for mutation carriers in *ASPM* and *SLC9A6* show marked phenotypic overlap with the brain malformations found in Case 6 and Case 7 arguing for the here identified mutations to be disease-causing.

While the identification of the *de novo* *BAZIA* mutation in Case 3 has been previously reported in one singleton in over 100,000 Europeans tested, Zaghlool et al. (2016), most recently identified a different *de novo* mutation in *BAZIA* (c.4043T > G; p.Phe1348Cys), in a patient with unexplained intellectual disability.

The amino acid substitution p.Arg1093Gln, identified in our patient, locates to a linker region between the BAZ-II and WKAZ domains (Figure 1). Fyodorov and Kadonaka (2002) deleted this region in *Drosophila* (AS 818–1010, corresponding to human AS 929–1103) and noticed an impaired interaction of Acf1 with ISWI, leading to defective chromatin assembly activity. The ISWI (imitation SWItch) family of remodeling complexes was first discovered in *Drosophila* and shown to be conserved in many other organisms (reviewed in Aydin, Vermeulen, & Lans, 2014). In mammals, seven different ISWI complexes have yet been identified and two, termed ACF and CHRAC, contain the *BAZIA* (ACF1) protein. The ACF-complex is built up from ACF1 and SMARCA5 and its activity alleviates barriers posed by heterochromatin, to enable DNA replication (Collins et al., 2002). The SMARCA5-ACF1 complex is also involved in regulation of transcription in concert with other histone modifiers and transcriptional regulators (Yasui, Miyano, Cai, Varga-Weisz, & Kohwi-Shigematsu, 2002). The CHRAC complex additionally includes histone-fold proteins CHRAC15 and CHRAC17, and these proteins were shown to facilitate ATP-dependent nucleosome sliding by ACF1/SMARCA5 (Kukimoto, Elderkin, Grimaldi, Oelgeschläger, & Varga-Weisz, 2004). The CHRAC complex is also recruited transiently to microirradiation-induced double-strand breaks (DSBs) and improves nonhomologous end joining and homologous recombination (Lan et al., 2010). Moreover, ACF1 has been implicated in G2/M checkpoint control in response to replication stress and DSBs (Sánchez-Molina et al., 2011) and in the interaction with transcription factor CCAAT/enhancer-binding protein beta (Steinberg et al., 2012). Hence, the p.Arg1093Gln variant may negatively influence all these functions.

Interestingly, the linker region affected by the p.Phe1348Cys substitution reported by Zaghlool et al. (2016), has no homologous region in *Drosophila Baz1a*, implicative that the p.Phe1348Cys substitution harboring region is overall less important for ACF1 protein function than the region harboring the here identified p.Arg1093Gln mutation. This might also explain the milder phenotype observed in the patient reported by Zaghlool et al. (2016) presenting with intellectual disability, epilepsy, ataxia, and hyper mobile joints, compared to the severe features of the patient reported here. As ACF1 is known to be involved in transcriptional repression of vitamin D3 receptor (VDR)-regulated genes through blocking the accessibility of the transcription factors to VDR in the absence of vitamin D3 (VD3) (Ewing, Attner, & Chakravarti, 2007),

Zaghlool et al. (2016) performed several experiments, showing that their patient displayed decreased binding of ACF1 to the promoter of the VDR-regulated gene *CYP24A1*. Using RNA sequencing, they further found that the mutation in their patient affects the expression of genes involved in several pathways including vitamin D metabolism, probably explaining the reduced vitamin-D (25-(OH)D) serum levels (70 nmol/l, normal range is 125–200 nmol/l) of their patient. In accordance, we measured the vitamin-D (25-(OH)D) serum levels in our patient, and were also able to show a reduced level of 54 nmol/l.

Consequently, we also investigated differential gene expression in Case 2 in comparison with the parents of Case 2 by RNA-Seq with Lexogen QuantSeq-3' mRNA. Obtained reads were processed with Subread (Liao et al., 2013), featureCounts (Liao et al., 2014) and edgeR (Robinson et al., 2010). We found 27 genes to be differentially expressed with an FDR < 5% (Supporting Information Table 2). Pathway analysis with Enrichr (<http://amp.pharm.mssm.edu/Enrichr>) (Chen et al., 2013; Kuleshov et al. 2016) revealed a possible implication in axon guidance (P 0.26). Database literature search with GeneCards (www.genecards.org) (Fishilevich et al., 2016) and UniProt (<http://www.uniprot.org/>) (The UniProt Consortium, 2015) showed that 10 out of these 27 genes are associated to cytoskeleton, integrin and synaptic related pathways, pinpointing to the relevance of *BAZIA* in neural development as supported by the findings of Zaghlool et al. (2016). As in situ hybridization in mouse embryos between E10.5 and E13.5 revealed *Baz1a* expression in the cloacal membrane and the central and peripheral nervous system, our study implicates an involvement of *BAZIA* not only in CNS anomalies but also in syndromic brain malformations.

5 | CONCLUSIONS

In syndromic brain malformations, WES is likely to identify causative mutations when chromosomal microarray analysis is unremarkable. Furthermore, our findings suggest *BAZIA* as a possible new candidate gene.

ACKNOWLEDGMENTS

We thank all patients and their families for their participation, as well as the German self-help organization for individuals with anorectal malformations (SoMA e.V.) for their assistance with recruitment. B. Stoffel-Wagner is acknowledged for vitamin D analysis.

ORCID

Heiko Reutter  <http://orcid.org/0000-0002-3591-5265>

REFERENCES

- Aldinger, K. A., Mosca, S. J., Tétéreault, M., Dempsey, J. C., Ishak, G. E., Hartley, T., ... Doherty, D. (2014). Mutations in *LAMA1* cause cerebellar dysplasia and cysts with and without retinal dystrophy. *American Journal of Human Genetics*, *95*(2), 227–234.
- Aasland, R., Gibson, T. J., & Stewart, A. F. (1995). The PHD finger: Implications for chromatin-mediated transcriptional regulation. *Trends in Biochemical Sciences*, *20*(2), 56–59.
- Aydin, Ö. Z., Vermeulen, W., & Lans, H. (2014). ISWI chromatin remodeling complexes in the DNA damage response. *Cell Cycle*, *13*(19), 3016–3025.
- Baraitser, M., & Winter, R. M. (1988). Iris coloboma, ptosis, hypertelorism, and mental retardation: a new syndrome. *Journal of Medical Genetics*, *25*(1), 41–43.
- Bond, J., Scott, S., Hampshire, D. J., Springell, K., Corry, P., Abramowicz, M. J., ... Woods, C. G. (2003). Protein-truncating mutations in *ASPM* cause variable reduction in brain size. *American Journal of Human Genetics*, *73*(5), 1170–1177.
- Chen, E. Y., Tan, C. M., Kou, Y., Duan, Q., Wang, Z., Meirelles, G. V., ... Ma'ayan, A. (2013). Enrichr: Interactive and collaborative HTML5 gene list enrichment analysis tool. *BMC Bioinformatics*, *14*, 128.
- Chitty, L. S., & Pilu, G. (2009). The challenge of imaging the fetal central nervous system: An aid to prenatal diagnosis, management and prognosis. *Prenatal Diagnosis*, *29*(4), 301–302.
- Collins, N., Poot, R. A., Kukimoto, I., García-Jiménez, C., Delleire, G., & Varga-Weisz, P. D. (2002). An ACF1-ISWI chromatin-remodeling complex is required for DNA replication through heterochromatin. *Nature Genetics*, *32*(4), 627–632.
- De Wit, M. C., Srebniak, M. I., Govaerts, L. C., Van Opstal, D., Galjaard, R. J., & Go, A. T. (2014). Additional value of prenatal genomic array testing in fetuses with isolated structural ultrasound abnormalities and a normal karyotype: A systematic review of the literature. *Ultrasound in Obstetrics & Gynecology*, *43*(2), 139–146.
- Doerks, T., Copley, R., & Bork, P. (2001). DDT—A novel domain in different transcription and chromosome remodeling factors. *Trends in Biochemical Sciences*, *26*(3), 145–146.
- Durinck, S., Spellman, P. T., Birney, E., & Huber, W. (2009). Mapping identifiers for the integration of genomic datasets with the R/Bioconductor package *biomaRt*. *Nature Protocols*, *4*(8), 1184–1191.
- Duyk, G. M., Kim, S. W., Myers, R. M., & Cox, D. R. (1990). Exon trapping: A genetic screen to identify candidate transcribed sequences in cloned mammalian genomic DNA. *Proceedings of the National Academy of Sciences of the United States of America*, *87*(22), 8995–8999.
- Dworschak, G. C., Draaken, M., Hilger, A. C., Schramm, C., Bartels, E., Schmiedeke, E., ... Reutter, H. (2015). Genome-wide mapping of copy number variations in patients with both anorectal malformations and central nervous system abnormalities. *Birth Defects Research. Part A, Clinical and Molecular Teratology*, *103*(4), 235–242.
- Ewing, A. K., Attner, M., & Chakravarti, D. (2007). Novel regulatory role for human Acf1 in transcriptional repression of vitamin D3

- receptor-regulated genes. *Molecular Endocrinology*, 21(8), 1791–1806.
- Fishilevich, S., Zimmerman, S., Kohn, A., Iny Stein, T., Olender, T., Kolker, E., ... Lancet, D. (2016). Genic insights from integrated human proteomics in GeneCards. Database (Oxford) 2016: baw030. Published online 2016 Mar 28. doi: 10.1093/database/baw030
- Fyodorov, D. V., & Kadonaga, J. T. (2002). Binding of Acf1 to DNA involves a WAC motif and is important for ACF-mediated chromatin assembly. *Molecular and Cellular Biology*, 22(18), 6344–6353.
- Gilfillan, G. D., Selmer, K. K., Roxrud, I., Smith, R., Kyllerman, M., Eiklid, K., ... Strømme, P. (2008). SLC9A6 mutations cause X-linked mental retardation, microcephaly, epilepsy, and ataxia, a phenotype mimicking Angelman syndrome. *American Society of Human Genetics*, 82(4), 1003–1010.
- Gray, K. A., Yates, B., Seal, R. L., Wright, M. W., & Bruford, E. A. (2015). Genenames.org: The HGNC resources in 2015. *Nucleic Acids Research*, 43(Database issue), D1079–D1085.
- Haack, T. B., Stauffer, C., Köpke, M. G., Straub, B. K., Kölker, S., Thiel, C., ... Prokisch, H. (2015). Biallelic mutations in *NBAS* cause recurrent acute liver failure with onset in infancy. *American Society of Human Genetics*, 97(1), 163–169.
- Hillman, S. C., McMullan, D. J., Hall, G., Togneri, F. S., James, N., Maher, E. J., ... Kilby, M. D. (2013). Use of prenatal chromosomal microarray: prospective cohort study and systematic review and meta-analysis. *Ultrasound in Obstetrics and Gynecology*, 41(6), 610–620.
- Jeng, L. B., Tarvin, R., & Robin, N. H. (2001). Genetic advances in central nervous system malformations in the fetus and neonate. *Seminars in Pediatric Neurology*, 8(2), 89–99.
- Jones, M. H., Hamana, N., Nezu, J. I., & Shimane, M. (2000). A novel family of bromodomain genes. *Genomics*, 63(1), 40–45.
- Kalter, H., & Warkany, J. (1983). Medical progress. Congenital malformations: etiologic factors and their role in prevention (first of two parts). *The New England Journal of Medicine*, 308(8), 424–431.
- Kariminejad, R., Lind-Thomsen, A., Tümer, Z., Erdogan, F., Ropers, H. H., Tommerup, N., ... Møller, R. S. (2011). High frequency of rare copy number variants affecting functionally related genes in patients with structural brain malformations. *Human Mutation*, 32(12), 1427–1435.
- Krutzke, S. K., Engels, H., Hofmann, A., Schumann, M. M., Cremer, K., Zink, A. M., ... Merz, W. M. (2016). Array-based molecular karyotyping in fetal brain malformations: Identification of novel candidate genes and chromosomal regions. *Birth Defects Research. Part A, Clinical and Molecular Teratology*, 106(1), 16–26.
- Kukimoto, I., Elderkin, S., Grimaldi, M., Oelgeschläger, T., & Varga-Weisz, P. D. (2004). The histone-fold protein complex CHRAC-15/17 enhances nucleosome sliding and assembly mediated by ACF. *Molecular Cell*, 13(2), 265–277.
- Kuleshov, M. V., Jones, M. R., Rouillard, A. D., Fernandez, N. F., Duan, Q., Wang, Z., ... Ma'ayan, A. (2016). Enrichr: A comprehensive gene set enrichment analysis web server 2016 update. *Nucleic Acids Research*, 44(W1), W90–W97.
- Kyte, J., & Doolittle, R. F. (1982). A simple method for displaying the hydrophobic character of a protein. *Journal of Molecular Biology*, 157(1), 105–132.
- Lan, L., Ui, A., Nakajima, S., Hatakeyama, K., Hoshi, M., Watanabe, R., ... Yasui, A. (2010). The ACF1 complex is required for DNA double-strand break repair in human cells. *Molecular Cell*, 40(6), 976–987.
- Liao, Y., Smyth, G. K., & Shi, W. (2013). The Subread aligner: Fast, accurate and scalable read mapping by seed-and-vote. *Nucleic Acids Research*, 41(10), e108.
- Liao, Y., Smyth, G. K., & Shi, W. (2014). FeatureCounts: An efficient general purpose program for assigning sequence reads to genomic features. *Bioinformatics*, 30(7), 923–930.
- Maksimova, N., Hara, K., Nikolaeva, I., Chun-Feng, T., Usui, T., Takagi, M., ... Onodera, O. (2010). Neuroblastoma amplified sequence gene is associated with a novel short stature syndrome characterised by optic nerve atrophy and Pelger-Huët anomaly. *Journal of Medical Genetics*, 47(8), 538–548.
- Mishra-Gorur, K., Çağlayan, A. O., Schaffer, A. E., Chabu, C., Hene-gariu, O., Vonhoff, F., ... Günel, M. (2014). Mutations in *KATNB1* cause complex cerebral malformations by disrupting asymmetrically dividing neural progenitors. *Neuron*, 84(6), 1226–1239.
- Noguchi, C., Rapp, J. B., Skorobogatko, Y. V., Bailey, L. D., & Noguchi, E. (2012). Swi1 associates with chromatin through the DDT domain and recruits Swi3 to preserve genomic integrity. *PLoS One*, 7(8), e43988.
- Peña, P. V., Davrazou, F., Shi, X., Walter, K. L., Verkhusha, V. V., Gozani, O., ... Kutateladze, T. G. (2006). Molecular mechanism of histone H3K4me3 recognition by plant homeodomain of ING2. *Nature*, 442(7098), 100–103.
- Pescosolido, M. F., Stein, D. M., Schmidt, M., El Achkar, C. M., Sabbagh, M., Rogg, J. M., ... Morrow, E. M. (2014). Genetic and phenotypic diversity of NHE6 mutations in Christianson syndrome. *Annals of Neurology*, 76(4), 581–593.
- Poretti, A., Boltshauser, E., & Huisman, T. A. (2014). Congenital brain malformations: An update on malformations of cortical development and infratentorial malformations. *Seminars in Neurology*, 34(3), 239–248.
- Rivière, J.-B., van Bon, B. W. M., Hoischen, A., Kholmanskikh, S. S., O'roak, B. J., Gilissen, C., ... Dobyns, W. B. (2012). *De novo* mutations in the actin genes *ACTB* and *ACTG1* cause Baraitser-Winter syndrome. *Nature Genetics*, 44(4), 440–444.
- Robinson, M. D., McCarthy, D. J., & Smyth, G. K. (2010). edgeR: a Bioconductor package for differential expression analysis of digital gene expression data. *Bioinformatics*, 26(1), 139–140.
- Sajan, S. A., Fernandez, L., Nieh, S. E., Rider, E., Bukshpun, P., Wakahiro, M., ... Sherr, E. H. (2013). Both rare and *de novo* copy number variants are prevalent in agenesis of the corpus callosum but not in cerebellar hypoplasia or polymicrogyria. *PLoS Genetics*, 9(10), e1003823.
- Sánchez-Molina, S., Mortusewicz, O., Bieber, B., Auer, S., Eckey, M., Leonhardt, H., ... Becker, P. B. (2011). Role for hACF1 in the G²/M damage checkpoint. *Nucleic Acids Research*, 39(19), 8445–8456.
- Schumann, M., Hofmann, A., Krutzke, S. K., Hilger, A. C., Marsch, F., Stienen, D., ... Reutter, H. (2016). Array-based molecular karyotyping in fetuses with isolated brain malformations identifies disease-causing CNVs. *Journal of Neurodevelopmental Disorders*, 8, 11.

- Shapiro, M. B., & Senapathy, P. (1987). RNA splice junctions of different classes of eukaryotes: Sequence statistics and functional implications in gene expression. *Nucleic Acids Research*, *15*(17), 7155–7174.
- Steinberg, X. P., Hepp, M. I., Fernández García, Y., Suganuma, T., Swanson, S. K., Washburn, M., ... Gutiérrez, J. L. (2012). Human CCAAT/enhancer-binding protein β interacts with chromatin remodeling complexes of the imitator switch subfamily. *Biochemistry*, *51*(5), 952–962.
- Stevenson, R. E., & Hunter, A. G. (2013). Considering the embryopathogenesis of VACTERL association. *Molecular Syndromology*, *4* (1–2), 7–15.
- The UniProt Consortium. (2015). UniProt: A hub for protein information. *Nucleic Acids Research*, *43*(D1), D204–D212.
- Verloes, A., Drunat, S., Pilz, D., & Di Donato, N. (2015). Baraitser-Winter cerebrofrontofacial syndrome. In: R.A. Pagon, M.P. Adam, H.H. Ardinger, S.E. Wallace, A. Amemiya, L.H.J. Bean, T.D. Bird, C.T. Fong, H.C. Mefford, R.J.H. Smith, K. Stephens, (Eds.), *Gene Reviews*[®]. Seattle, WA: University of Washington, Seattle.
- Wapner, R. J., Martin, C. L., Levy, B., Ballif, B. C., Eng, C. M., Zachary, J. M., ... Jackson, L. (2012). Chromosomal microarray versus karyotyping for prenatal diagnosis. *The New England Journal of Medicine*, *367*(23), 2175–2184.
- Yasui, D., Miyano, M., Cai, S., Varga-Weisz, P., & Kohwi-Shigematsu, T. (2002). SATB1 targets chromatin remodelling to regulate genes over long distances. *Nature*, *419*(6907), 641–645.
- Zaghlool, A., Halvardson, J., Zhao, J. J., Etemadikhah, M., Kalushkova, A., Kanska, K., ... Feuk, L. (2016). A role for the chromatin-remodeling factor BAZ1A in neurodevelopment. *Human Mutation*, *37*(9), 964–975.
- Zeng, L., & Zhou, M. M. (2002). Bromodomain: an acetyl-lysine binding domain. *FEBS Letter*, *513*(1), 124–128.

SUPPORTING INFORMATION

Additional Supporting Information may be found online in the supporting information tab for this article.

Table S1. Pipeline and filter parameters used for WES

Table S2. Differentially expressed genes in Case 2 and the parents of Case 2

Figure S1. Analysis of a possible splice site effect of ACTB (c.802G>C)

Figure S2. X chromosome inactivation patterns at the HUMARA locus

How to cite this article: Weitensteiner V, Zhang R, Bungenberg J, et al. Exome sequencing in syndromic brain malformations identifies novel mutations in *ACTB*, and *SLC9A6*, and suggests *BAZ1A* as a new candidate gene. *Birth Defects Research*. 2018;110:587–597. <https://doi.org/10.1002/bdr2.1200>